Supplementary Information for the article entitled: Gradual Regime Shifts in Fairy Circles

Yuval R. Zelnik,[1] Ehud Meron,[1,2] and Golan Bel[1]

[1]*Department of Solar Energy and Environmental Physics, BIDR, Ben-Gurion University of the Negev, Sede Boqer Campus 8499000, Israel*

[2]*Department of Physics, Ben-Gurion University, Beer Sheva, 84105, Israel*

Derivation of the simplified model

We present the derivation of the simplified model that we use and analyze in the main text. Our starting point is the vegetation model of Gilad et al. [1] that includes three pattern-forming feedbacks. Using the characteristics of the fairy circles ecosystem, we explain the assumptions and approximations that allow us to replace the integrals of the root-augmentation feedback with simpler algebraic terms and to decouple the aboveground water dynamics from the soil-water and vegetation dynamics.

The dryland vegetation model of Gilad et al. [1] describes the coupled dynamics of the areal densities of vegetation biomass (B), soil water (W) and surface water (H), all having the dimension of mass per unit area. The dynamics is described with a temporal resolution that is smaller than the typical time scale for changes in the biomass (dictated by the biomass growth rate, mortality and dispersion rate) but is large enough to allow averaging the intermittent nature of the precipitation. The spatial scale resolution is larger than the scale of a single plant (in order to allow the description of a continuous vegetation density) but smaller than the typical patch size. Restricting our interest to flat terrains, the model reads:

$$B_T = G_B B(1 - B/K) - MB + D_B \nabla^2 B \tag{1a}$$

$$W_T = IH - N(1 - RB/K)W - G_W W + D_W \nabla^2 W \tag{1b}$$

$$H_T = P - IH + D_H \nabla^2 (H^2)\,, \tag{1c}$$

where

$$G_B(\mathbf{X},T) = \Lambda \int_\Omega G(\mathbf{X},\mathbf{X}',T) W(\mathbf{X}',T) \mathbf{dX}' \tag{2a}$$

$$G_W(\mathbf{X},T) = \Gamma \int_\Omega G(\mathbf{X},\mathbf{X}',T) B(\mathbf{X}',T) \mathbf{dX}' \tag{2b}$$

$$G(\mathbf{X},\mathbf{X}',T) = \frac{1}{2\pi S_0^2} \exp\left[-\frac{|\mathbf{X}-\mathbf{X}'|^2}{2S_0^2(1+EB(\mathbf{X},T))^2} \right] \tag{2c}$$

$$I = A\frac{B(\mathbf{X},T)+Qf}{B(\mathbf{X},T)+Q} \tag{2d}$$

The terms G_B and G_W involve integration over a root kernel (G) that represents the spatial extent of the root zone in the lateral directions. Applying the model to perennial grasses, e.g. *Stipagrostis Ciliata* (common in the fairy circle ecosystem), which form patterns with a typical length scale of $10m$ [2] and have a root girth of approximately $0.5m$ [3], allows us to assume that the kernel function is much narrower than the biomass and soil-water distributions. Under this condition, we can approximate the kernel by a Dirac delta function. Formally, this is done by taking the limit $S_0 \to 0$ in Eq. 2c, where S_0 represents the lateral root-zone size of a seedling. Following this approximation, we may replace the integrals of Eqs. (2c) by the algebraic forms:

$$G_B(\mathbf{X},T) = \Lambda W(\mathbf{X},T)(1+EB(\mathbf{X},T))^2; \tag{3a}$$

$$G_W(\mathbf{X},T) = \Gamma B(\mathbf{X},T)(1+EB(\mathbf{X},T))^2. \tag{3b}$$

The fairy circle ecosystem consists of sandy soil. This soil type is characterized by a high rate of surface water infiltration that is comparable to the infiltration rate in vegetated soil. To account for the absence of a significant infiltration contrast between bare and vegetated soil, we set $f = 1$. The infiltration rate then becomes a constant, $I = A$, independent of the biomass B, and the equation for the surface water variable H decouples from those for B and W. This equation has a single stationary uniform solution, $H_0 = P/I$, which is always linearly stable. Since H is the fastest variable, we can assume that, on the much slower time scales over which B and W significantly change, it has already equilibrated at H_0. Inserting the solution $H = H_0$

into the equation for W, we obtain the two-variable model:

$$B_T = \Lambda W(\mathbf{X}, T)(1 + EB(\mathbf{X}, T))^2 B(1 - B/K) - MB + D_B \nabla^2 B \tag{4a}$$

$$W_T = P - N(1 - RB/K)W - \Gamma B(\mathbf{X}, T)(1 + EB(\mathbf{X}, T))^2 W + D_W \nabla^2 W. \tag{4b}$$

In the biomass equation, Λ is the biomass growth rate coefficient, K is the maximal standing biomass, E is a measure for the root-to-shoot ratio, M is the mortality rate, and D_B represents the seed dispersal or clonal growth rate. In the soil-water equation, P is the precipitation rate, N is the evaporation rate, R is a dimensionless factor representing a reduction of the evaporation rate due to shading, Γ is the water-uptake rate coefficient, and D_W is the effective soil-water diffusivity in the lateral (X, Y) directions, assumed to be a constant, independent of the state variables, that represents linear diffusion[1]. We refer the reader to an earlier publication[1] for additional information about the original model. The model considered here (Eqs. (4)) predicts, in addition to the states shown and discussed in the main paper, the appearance of spotted and patterned states under low precipitation rates as shown in Fig. 1.

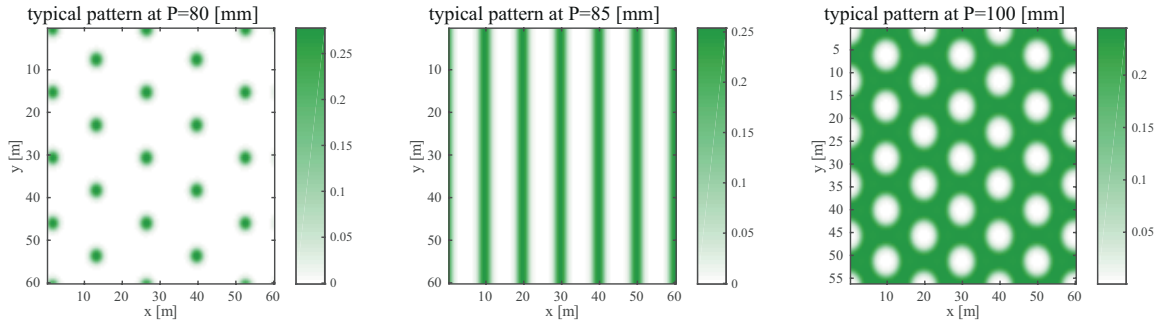

FIG. 1: Patterns predicted by the model for low precipitation rates.

Sensitivity Analysis

In order to test the sensitivity of the results (presented in the main text) to the set of parameters, we first write the model in a dimensionless form. Thereby, we reduce the number of parameters and simplify the analysis.

parameter	$+10\%$	-10%
λ	0.8913	1.1269
η	1.0179	0.9664
ν	1.0604	0.9404
ρ	1.0183	0.9819
δ_w	1.0556	0.9413

TABLE I: Relative change in the existence range of the hybrid states (snaking range), due to varied parameters compared to those used in the main text. In each case, one parameter is changed by either $+10\%$ or -10%, and the relative existence range is shown.

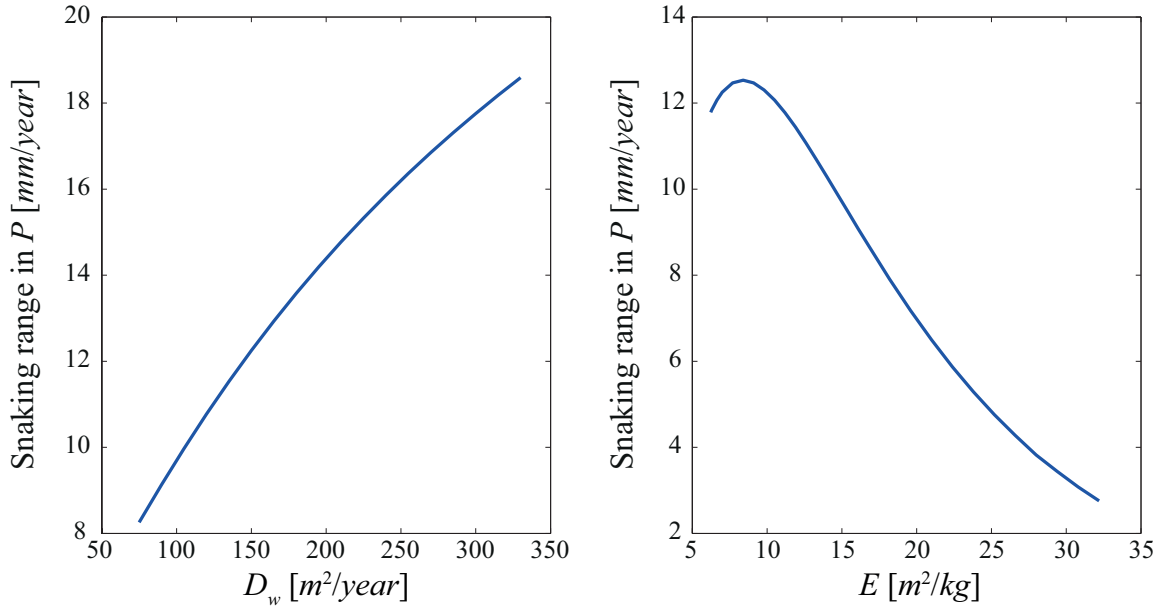

FIG. 2: The range of precipitation rates, P, for which stable hybrid states exist, as a function of either D_W (left) or E (right).

Equations (4) describe the dynamics of the aboveground biomass (B) and the soil water (W) in a dimensional form. Translation of the model equations to a dimensionless form is achieved

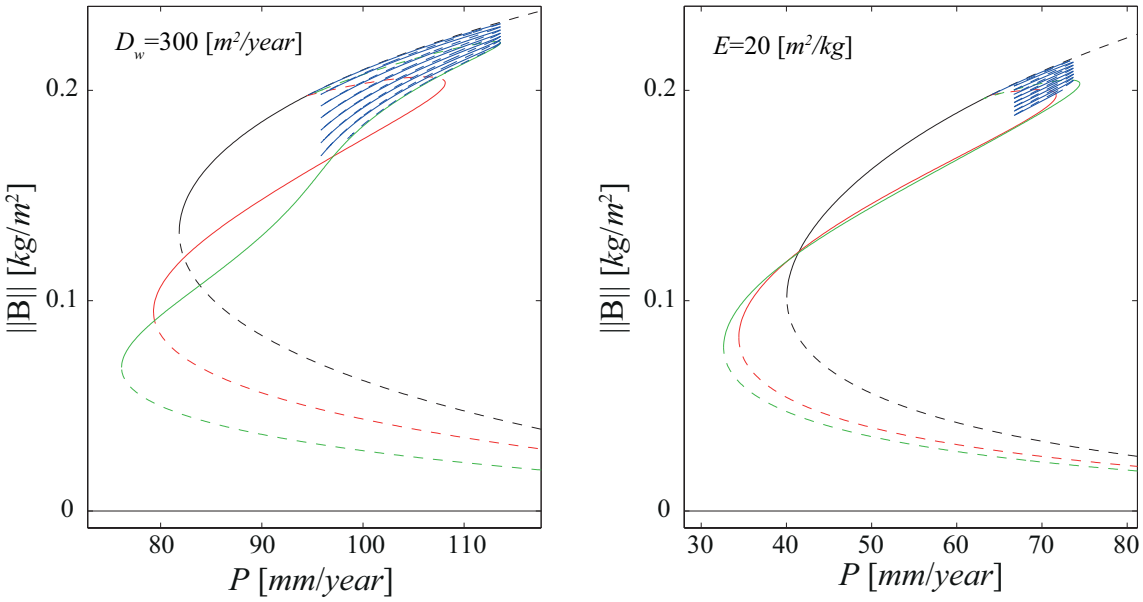

FIG. 3: Bifurication graphs for two sets of parameters. On the left panel, D_W was changed to 300 [$m^2/year$], while on the right panel, E was changed to 20 [m^2/kg]. Uniform states (bare soil and uniform vegetation) are shown in black, two periodic states are shown in red and green, and the hybrid states are shown in blue.

by rescaling the state variables B, W and the space and time coordinates as follows:

$$b = \frac{B}{K}; w = \frac{W\Lambda}{K\Gamma}; t = MT; x = X\sqrt{M/D_B}\,. \tag{5}$$

In terms of these dimensionless quantities, the model reads:

$$\partial_t b = \lambda w b(1+\eta b)^2(1-b) - b + \nabla^2 b\,, \tag{6}$$

$$\partial_t w = p - \nu w(1-\rho b) - \lambda w b(1+\eta b)^2 + \delta_w \nabla^2 w\,. \tag{7}$$

The dimensionless parameters here are related to their dimensional counterparts by the following relations:

$$\lambda = \frac{K\Gamma}{M}; \quad \eta = EK; \quad p = \frac{\Lambda P}{K\Gamma M}; \quad \nu = \frac{N}{M}; \quad \rho = R; \quad \delta_w = \frac{D_W}{D_B}\,. \tag{8}$$

We are thus left with only six parameters, for which we use p as the main bifurcation parameter, and as such, its value changes throughout our analysis. The basis for the main results is

the existence of stable hybrid states; therefore, we tested the conditions under which they occur and their existence range (range of precipitation rate, p). We changed the other five parameters, one at a time, within $\pm 10\%$ of their value. We found that in all cases, the hybrid states exist, with their existence range slightly changing. The relative changes in their existence range are shown in Table I.

As can be seen, the parameter λ has the strongest effect on the snaking range. The parameters η and δ_w control the pattern-forming feedback in our model [4]. Therefore, we present a more thorough analysis of their effect on the snaking range. In Fig. 2, we show the snaking range as a function of either D_W (left panel) or E (right panel). Fig. 3 shows two examples of the bifurcation diagram for a relatively big change in one of these parameters.

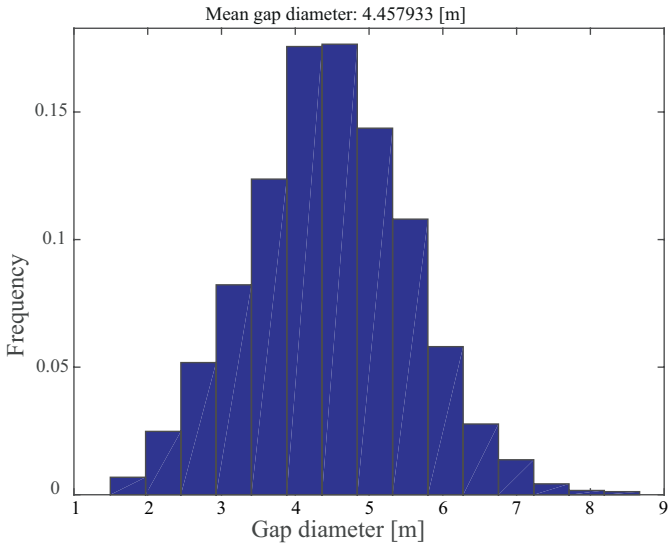

FIG. 4: Histogram of the FCs size in the regions covered by the satellite images that were analyzed.

In addition to the sensitivity of the snaking range to the parameters the size of the gaps and the distance between neighboring gaps are also affected by the parameters. The histogram of the FC sizes, in the regions for which the satellite images were analyzed, is shown in Fig. 4. In Fig. 5 we show the average size of the FCs and the average distance between them as predicted by our model for constant precipitation rate of $P = 102[mm/yr]$ and for a range of the feedback control parameters D_w and E. It is shown that there is a range of values of these parameters

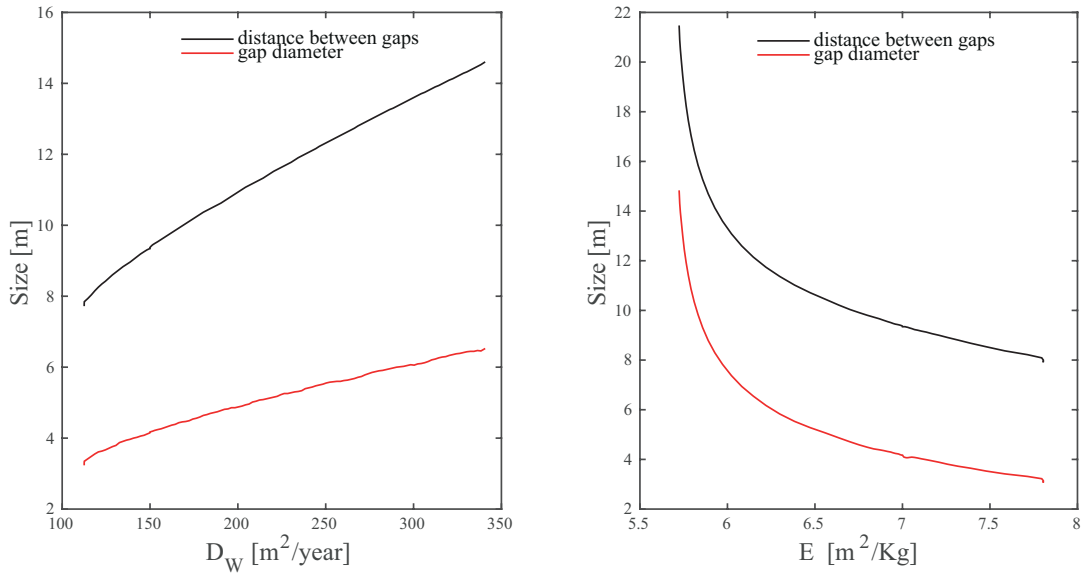

FIG. 5: The average gap size and distance between neighboring gaps vs. the parameters D_w (left panel) and E (right panel) as predicted by the model for constant $P = 102[mm/yr]$.

that correspond to the FCs size observed in the field. The range of possible values for these parameters, which have not been measured directly in the field, may be estimated from these graphs.

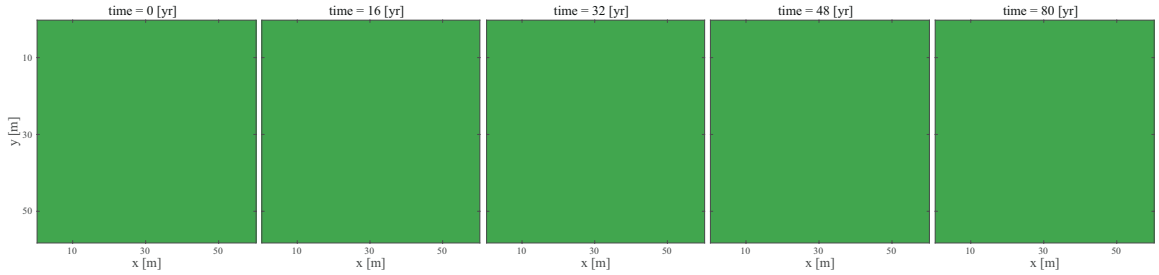

FIG. 6: The response of 2D uniform vegetation to periodic short droughts. No regime shift takes place even though the system is subjected to the same rainfall regime as the hybrid state in figure 4**B**. The rainfall regime represents periodic one-year droughts with $P = 81[mm/yr]$, followed by 15 years of $P = 102[mm/yr]$. The simulated domains are $60[m] \times 56[m]$.

Predicted response of uniform vegetation to a series of droughts

In the main paper, we showed that the response of vegetation to a series of droughts or spates depends on the initial condition. To complement the information we present in Fig. 6 the response of a uniform vegetation to a series of droughts.

---

[1] E. Gilad, J. von Hardenberg, A. Provenzale, M. Shachak, and E. Meron. A Mathematical Model for Plants as Ecosystem Engineers. *J. Theor. Biol.*, 244:680, 2007.

[2] M. D. Picker, V. Ross-Gillespie, K. Vlieghe, and E. Moll. Ants and the enigmatic namibian fairy circles–cause and effect? *Ecological Entomology*, 37(1):33–42, 2012.

[3] G. F. Midgley and F. van der Heyden. *The Karoo: Ecological Patterns and Processes*, chapter 6, Form and Function in perennial plants, pages 91–106. Cambridge University Press, Cambridge, UK, 1999.

[4] S. Kinast, Y. R. Zelnik, G. Bel, and E. Meron. Interplay between turing mechanisms can increase pattern diversity. *Phys. Rev. Lett.*, 112:078701, 2014.